



UvA-DARE (Digital Academic Repository)

Cardiac microvascular dysfunction

Insights from COVID-19, myocardial infarction, and anthracycline-induced cardiotoxicity

Jiang, Z.

Publication date

2026

[Link to publication](#)

Citation for published version (APA):

Jiang, Z. (2026). *Cardiac microvascular dysfunction: Insights from COVID-19, myocardial infarction, and anthracycline-induced cardiotoxicity*. [Thesis, fully internal, Universiteit van Amsterdam].

General rights

It is not permitted to download or to forward/distribute the text or part of it without the consent of the author(s) and/or copyright holder(s), other than for strictly personal, individual use, unless the work is under an open content license (like Creative Commons).

Disclaimer/Complaints regulations

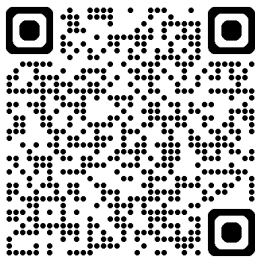
If you believe that digital publication of certain material infringes any of your rights or (privacy) interests, please let the Library know, stating your reasons. In case of a legitimate complaint, the Library will make the material inaccessible and/or remove it from the website. Please Ask the Library: <https://uba.uva.nl/en/contact>, or a letter to: Library of the University of Amsterdam, Secretariat, P.O. Box 19185, 1000 GD Amsterdam, The Netherlands. You will be contacted as soon as possible.

Chapter 6

N^ε-(carboxymethyl)lysine-modified albumin exacerbates doxorubicin-induced NOX5-dependent oxidative stress in endothelial cells

Zhu Jiang *MEng*, Ingeborg.S.E.Waas *BSc*, Suat Simsek *MD PhD*,
Casper G. Schalkwijk *PhD*, Joris J.T.H. Roelofs *MD PhD*, Hans W.M. Niessen
MD PhD, Paul A.J. Krijnen *PhD*

Running title: CML amplifies NOX5-mediated oxidative stress



Published in :

Biochemical and Biophysical Research Communications. Volume 796, 18 January 2026,153135.

1

2

3

4

5

6

7

8

9

10

Abstract

Introduction Doxorubicin (Dox), a potent chemotherapeutic agent, is associated with cardiovascular complications. Dox-induced cardiotoxicity involves accumulation of N^ε-(carboxymethyl)lysine (CML) and activation of its receptor, RAGE (receptor for advanced glycation end-products) in the cardiac microvasculature, potentially driven by NADPH oxidase (NOX)-mediated oxidative stress. NOX5 is a critical contributor to endothelial dysfunction. But its role, alongside extracellular CML, in Dox-induced vascular dysfunction remains unclear. This study investigated the impact of Dox and CML-bovine serum albumin (CML-BSA) on endothelial oxidative stress, and the involvement of NOX5 therein.

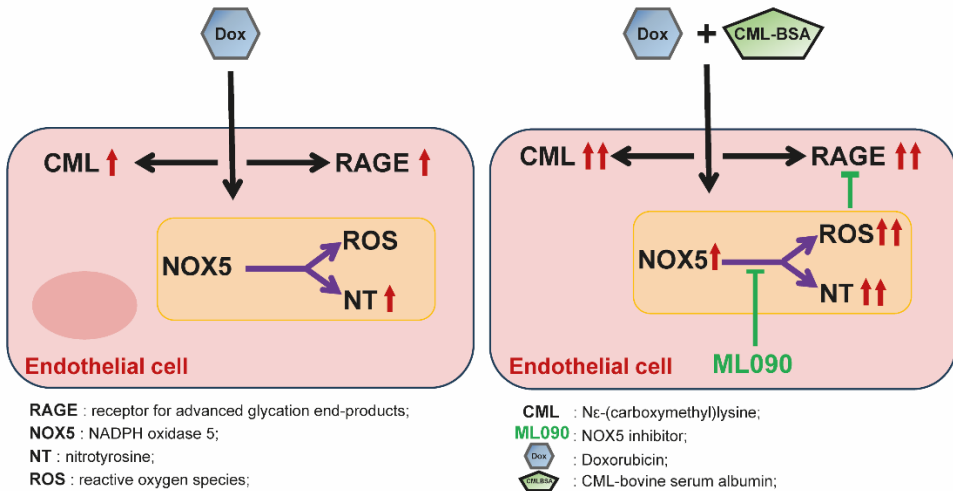
Materials and methods Human umbilical vein endothelial cells (HUVECs) were treated with Dox and/or CML-BSA for 6h, with or without NOX5 inhibitor ML090. Cell viability was assessed by MTT assay. Reactive oxygen species (ROS), Nitrotyrosine (NT), NOX5, RAGE and CML were visualized and quantified using confocal immunofluorescence imaging and intensity analysis. Subcellular NOX5 localization was confirmed via immunofluorescence. Golgi apparatus morphology was analyzed using electron microscopy.

Results Dox induced endogenous CML generation and the cellular CML levels were increased further by CML-BSA. Dox significantly reduced cell viability, which was not affected further by CML-BSA. Combined Dox and CML-BSA treatment increased RAGE expression and nitrosative/oxidative stress, evidenced by increased ROS, NT, and NOX5 levels, which was suppressed by ML090. NOX5 localized primarily to the Golgi apparatus, which was fragmented after Dox exposure.

Discussion and conclusion Extracellular CML-BSA exacerbated Dox-induced CML accumulation and NOX5-related oxidative stress in endothelial cells. These findings suggest elevated circulating CML may worsen Dox-induced cardiovascular toxicity, aligning with clinical observations in diabetic patients.

Keywords: Doxorubicin; N^ε-(carboxymethyl)lysine; NOX5; Oxidative stress; Human umbilical vein endothelial cells;

Graphical Abstract



Highlights:

- CML-BSA enhances Dox-induced endothelial dysfunction
- Dox and CML-BSA synergistically increase NOX5 and RAGE in endothelial cells
- NOX5 inhibition mitigates Dox- and CML-induced oxidative and nitrosative stress
- Golgi-localized NOX5 links stress to organelle damage
- Circulating CML may amplify Dox-induced vascular toxicity via NOX5 activation

1. Introduction

Doxorubicin (Dox) is a potent anthracycline chemotherapeutic compound for treating childhood and adult malignancies, including hematological cancers such as leukemias and lymphomas, and solid tumors such as breast cancer and sarcomas^[1]. Its clinical utility is limited by cardiotoxicity, affecting 9-18% of cancer patients and reaching an incidence of 26% for congestive heart failure incidence at cumulative dose ≥ 550 mg/m², with higher doses conferring exponentially greater risk^[2,3]. The cardiotoxicity is associated with the development of cardiovascular disease^[4,5], with established toxic effects on endothelial cells (EC), that can lead to long term impairment of cardiac and vascular function^[6].

Dox has been shown to induce damage and dysfunction of EC both in vitro as in animal models in vivo, as indicated by increased production of pro-inflammatory cytokines and adhesion molecules, lowered nitric oxide (NO) availability and increased cell death^[7]. A major contributor to Dox-induced endothelial dysfunction is oxidative stress, evidenced by observed significant increases in reactive oxygen species (ROS), myeloperoxidase (MPO) and reactive nitrogen species (RNS) in EC both in vitro and in vivo^[8-10].

Oxidative stress in EC is intrinsically linked to advanced glycation end products (AGEs), as increased oxidative stress enhances AGE formation. AGEs are produced through non-enzymatic reactions of sugars with proteins, lipids and nucleic acids under conditions of oxidative stress and/or hyperglycemia, and can form both in the blood and in tissues, including in EC^[11]. In addition, exposure of EC to AGEs further enhances oxidative stress, partly through interaction with their primary receptor, RAGE^[12,13].

There is increasing evidence supporting an important role for AGEs in Dox-induced cardiovascular toxicity. N^ε-(carboxymethyl)lysine (CML) is one of the most abundant AGEs associated with aging and disease^[14,15]. CML has been closely linked to vascular pathology, with elevated circulating levels correlating with cardiovascular events^[16] and local deposition detected in blood vessels, for instance contributing to atherosclerosis through both RAGE-dependent and RAGE-independent pathways^[17,18]. These features highlight CML as a key mediator of endothelial dysfunction. Previously, we showed increased accumulation of the AGE N^ε-(carboxymethyl)lysine (CML) in cardiac microvascular EC in Dox-treated mice^[19]. Moreover, Dox treatment of rats was shown to induce accumulation of CML and another AGE pentosidine in cardiomyocytes, which correlated significantly with decreased heart function and increased cardiac damage^[20], and with myocardial fibrosis, inflammation, oxidative stress and mitochondrial damage^[21], which could be ameliorated by AGE-inhibitors aminoguanidine and pyridoxamine. Lastly, Dox-induced aortic stiffening in mice was accompanied with increased accumulation of AGEs in the aortic wall^[22].

Interestingly, pre-exposure of human cardiomyocytes to exogenous CML in vitro exacerbated the toxic effects of Dox^[23]. In line herewith, blockage or knockout of RAGE in mice was recently shown to reduce Dox-induced cardiac damage and

function loss^[24]. These results suggest that extracellular AGEs can enhance Dox-induced cytotoxicity. However, whether this is also the case in EC is unknown.

The primary source of ROS within EC are NADPH oxidases (NOXes). NOXes play a putative role in endothelial dysfunction^[25], including in AGEs-induced oxidative stress^[26]. Of the four NOX isoforms (NOX1,2,4 and 5) expressed in EC, NOX5 is arguably the least well studied, partly because the NOX5 gene is not expressed in commonly used rodent animal models. Contrary to NOX1,2,4, NOX5 functions independently of the p22phox subunit and is regulated by intracellular calcium levels. Notably, increased NOX5 expression was observed in EC of atherosclerotic lesions of patients with coronary artery disease^[27] and in the cardiac microvasculature of myocardial infarction patients^[28] and patients with severe COVID19^[29]. Moreover, NOX5 overexpression promoted EC dysfunction in human brain microvascular EC^[30], pointing to a role of NOX5 in EC dysfunction.

However, whether NOX5 plays a role in Dox-induced EC dysfunction, as well as the effect thereon of extracellular AGEs, remains unknown. To investigate the effect of extracellular CML, CML-modified bovine serum albumin (CML-BSA)^[31,32] was employed to assess the effects of Dox and extracellular AGEs on cell viability, oxidative and nitrosative stress and RAGE expression in EC, with a focus on the role of NOX5 herein.

2. Materials and Methods

2.1 Materials and cells

Chemicals and reagents used in this study are listed in **Table 1**. Human Umbilical Vein Endothelial Cells (HUVECs) were obtained from ScienCell (#8000, Carlsbad, CA, USA). The HUVECs were cultured in Endothelial Cell Medium with endothelial cell growth supplement, antibiotic solution, and fetal bovine serum (FBS, #1001, ECM; ScienCell). Doxorubicin hydrochloride (#DM1515, Sigma-Aldrich, St. Louis, MO, USA) was prepared in as a stock solution by dissolving it in Dimethylsulfoxide (DMSO) and stored at -80°C. CML-modified bovine serum albumin (CML-BSA) was obtained from MBL CircuLex.

Table 1. Chemicals and reagents used in this study

Name	Source	Code number or CAS number
Endothelial Cell Medium (ECM)	ScienCell (USA)	#1001
Endothelial cell growth supplement	ScienCell (USA)	#1052
Penicillin/streptomycin solution	ScienCell (USA)	#0503
Fetal bovine serum	ScienCell (USA)	#0025
N ^ε -(carboxymethyl)lysine (CML)-albumin	MBL CircuLex	#CY-R2052
CellROX™ Deep Red Reagent	Thermo Scientific (USA)	C10422
Prolong Gold antifade reagent	Thermo Scientific (USA)	P36934
5,12-dihydroquinoxalino(2,3-b)quinoxaline (ML090)	Sigma-Aldrich (St. Louis, MO, USA)	S920371
Doxorubicin hydrochloride	Sigma-Aldrich (St. Louis, MO, USA)	25316-40-9 (D1515-10mg)
Thiazolyl Blue Tetrazolium Bromide (MTT)	Sigma-Aldrich (St. Louis, MO, USA)	298-93-1
Dimethylsulfoxide (DMSO)	Sigma-Aldrich (St. Louis, MO, USA)	67-68-5

2.2 Cell culture

The HUVECs were cultured in ECM at 37°C in a humidified 5% CO₂ environment. HUVECs in passage 2-4 were used in all experiments, all experiments were performed in complete endothelial cell medium without serum starvation^[33]. For experiments, the cells were cultured in 24- and 96-well plates. For immunofluorescence analysis experiments the cells were cultured in 24-well plates on glass coverslips. When the cells reached approximately 90% confluence, they were exposed for 6 hours to ECM containing either Dox (final concentration = 10 μM), or CML-BSA (final concentration = 20 μg/ml), or a combination of Dox (10 μM) and CML-BSA (20 μg/ml). The concentration of CML-BSA (20 μg/ml) exceeds mean serum levels reported in human (~0.3–0.5 μg/ml, >1 μg/ml in individuals with chronic conditions^[34,35]), but was chosen to ensure sufficient in vitro exposure given that only a fraction of lysine residues on BSA are CML-

modified. Notably, FBS contains a substantial amount of BSA (in the order of 2.5 mg/ml^[36]), which corresponds to approximately 250 µg/ml BSA in the used endothelial culture medium. This excess of non-glycated BSA served as a BSA control. As Dox was dissolved in DMSO, ECM containing an equivalent concentration of DMSO as present in the Dox supplemented medium, was used as a control.

In experiments involving the NOX5 inhibitor 5,12-dihydroquinoxalino(2,3-b)quinoxaline (ML090)^[37], the inhibitor was added to the ECM at a final concentration of 0.01 µM, 30 minutes prior to addition of Dox and/or CML-BSA.

2.3 (Immuno)fluorescence staining

For immunofluorescence stainings, the cells were fixed after treatment with 4% paraformaldehyde for 10 minutes at room temperature (RT) and subsequently permeabilized using 0.1% (v/v) Trion X-100 in PBS for 10 min. After extensive washing with PBS, the cells were blocked with a solution of 1% BSA and 0.1% NaN₃ in PBS. The cells were then incubated with primary antibodies: mouse-anti-CML^[38], rabbit-anti-Nitrotyrosine (Chemicon; AB5411, 1:500 dilution), mouse-anti-GM130 (abcam; ab169276, 1:100), goat-anti-RAGE (ab5484, 1:100 dilution) and/or rabbit-anti-NOX5 (abcam; ab191010, 1:1000 dilution) for 2 hours at RT. After washing 3 times with PBS, the cells were incubated with secondary antibodies: donkey-anti-rabbit IgG(H+L) A488 (for NOX5 and nitrotyrosine, Jackson immune research; 711-545-152, 1:500 dilution), goat-anti-mouse IgG(H+L) A488 (for GM130, Thermo Fisher Scientific; A11029, 1:500 dilution), donkey-anti-goat IgG(H+L) A633 (for RAGE, Thermo Fisher Scientific; A21082, 1:500 dilution) or goat-anti-mouse IgG(H+L) A647 (for CML, Thermo Fisher Scientific; A28181, 1:500 dilution) for 1 hour at RT. Hoechst (1:1000 dilution) was used for counterstaining cells. For superoxide detection, CellROX™ Deep Red Reagent (Thermo Fisher Scientific; C10422) was added to the treated cells at a final concentration of 5 µM at 37°C, 30 minutes before fixation in 4% paraformaldehyde, Hoechst (Thermo Fisher Scientific; 62249; 1:1000 dilution) was used for counterstaining cells simultaneously. After staining, the cells were covered with Prolong Gold antifade reagent (Thermo Fisher Scientific; P36934) and the coverslips were mounted onto glass slides. Cells that were stained without primary antibody and without any antibody served as negative controls.

A Leica DMi8 inverted microscope equipped with a Leica TCS SP8 X DLS camera was used to image the slides at 400× and 600× magnification. 8-15 pictures were taken from each individual sample per staining for analysis. For each marker, the fluorescent intensity as well as the cell numbers were determined using ImageJ2 and Qupath-0.5.0 software. The fluorescent intensity was divided by number of cells to obtain the mean fluorescence intensity.

2.4 MTT Assay

Thiazolyl Blue Tetrazolium Bromide (MTT) assays^[39,40] were performed after 6 h of exposure to provide an readout of metabolic viability (mitochondrial dehydrogenase activity) under acute treatment conditions. The cells were cultured in 96-well plates, MTT was dissolved in PBS to a stock concentration of 5 mg/mL and filtered through a 22 µm filter to sterilize. After treatment of the cells, 10 µL of prepared MTT solution was added to the medium and incubated at 37°C for 3 hours. After conformation of purple formazan formation under a light microscope, the medium was removed from the wells and 50 µL DMSO was added to each well to fully solubilize the formazan, absorbance at 570 nm was subsequently measured using a CLARIO star Plus microplate reader.

2.5 Transmission electron microscopy analysis

HUVECs were cultured in T75 flasks and treated with Dox or an equivalent concentration of DMSO as a control for 6 hours. Following the treatment, an equal volume of freshly prepared 2x fixative (1% Gluteraldehyde and 4% paraformaldehyde in phosphate buffer, pre-warmed to RT) was added directly to the culture medium within the T75 flask and fixation was conducted for 4 hours at RT. The cells were then rinsed with PBS, collected using cell scrapers, post-fixed with 1% osmium tetroxide (OsO₄) solution to enhance membrane contrast, and subsequently dehydrated through a series of ethanol. The dehydrated cells were pelleted and embedded in epon epoxy resin at 65°C to create solid embedding blocks. Ultra-thin sections were prepared using a Leica Ultracut FC6 microtome, mounted onto copper grids, and stained with uranyl acetate. 10-15 cells from each individual sample were imaged at 30000× magnification. Imaging was performed using a transmission electron microscope at 120 kV (Talos 120 with Ceta 16 M camera and Tecnai T12 with Velata and Xarosa camera).

2.6 Statistics

GraphPad Prism (version 9, San Diego, CA, USA) was used for the design and generation of graphs. Statistical analyses were conducted using GraphPad Prism, SPSS (version 26.0, Armonk, NY, USA). Each experiment was replicated a minimum of three times. Two-group comparisons were analyzed using unpaired t-tests, while comparisons among three or more groups were analyzed using one-way analysis of variance (ANOVA) followed by Tukey's post hoc test for multiple comparisons. Data were presented using mean \pm [standard deviation (SD)], *p* value below 0.05 was considered statistically significant.

3. Results

3.1 Effects of Dox on CML formation, RAGE expression and accumulation of exogenous CML-BSA in HUVECs

To study the effects of Dox on the formation of CML in endothelial cells, HUVECs were treated with 10 μ M Dox for 6 h. Pharmacokinetic studies have shown that the peak plasma concentration of Dox in patients exceeds 10 μ M^[41], followed by a gradual decline over time. In our pilot experiments (data not shown), short-term exposure (\leq 6-8 hours) to 10 μ M Dox resulted in limited cell death (<15%), thereby enabling the observation of acute endothelial stress rather than extensive cytotoxicity. In DMSO-treated cells, low levels of CML were detected, whereas Dox-treated cells exhibited increased level of CML, as demonstrated by fluorescent staining (**Figure 1A**). The Dox-induced formation of CML in HUVECs was primarily localized within the nucleus and peri-nuclear areas (**Figure 1A**) and the CML levels in Dox-treated HUVECs were 2.50 ± 1.18 -fold higher than in DMSO-treated cells ($p < 0.05$; **Figure 1B**). For visualization, due to the faint CML signal in control and Dox-only conditions, also digitally enhanced representative images are shown. However, all quantifications were performed on raw, non-enhanced images acquired under identical settings.

To study the effects of Dox on accumulation of exogenous CML in endothelial cells, HUVECs were cultured with/without 10 μ M Dox and with/without 20 μ g/mL CML-BSA for 6 h. Especially in the Dox-treated cells, presence of exogenously added CML-BSA in the culture medium resulted in elevated CML accumulation in endothelial cells, that was found both intracellularly and on the plasma membrane

(**Figure 1A**). Both in DMSO- and Dox-treated cells, addition of CML-BSA to the culture medium resulted in significantly increased cellular CML levels, predominantly localized to cell membrane and cytoplasmic regions, (respectively 2883 ± 1204 -fold and 13941 ± 10535 fold higher than in DMSO-treated cells ($p < 0.05$)). However, this accumulation of CML was higher in Dox-treated cells compared to DMSO-treated (4.8 ± 2.38 -fold $p < 0.05$; **Figure 1B**). The DMSO did not significantly affect endogenous formation of CML, nor CML accumulation in the presence of CML-BSA compared to HUVECs cultured in ECM alone (data not shown).

Additionally, the effects of Dox and CML-BSA on RAGE expression in HUVECs were investigated. Fluorescence staining showed RAGE primarily localized in the peri-nuclear region and cytoplasm, with some plasma membrane staining (**Figure 1C**). Dox treatment significantly increased RAGE expression compared to the DMSO group, with a notable enhancement in cytoplasmic RAGE expression (1.81 ± 0.62 -fold, $p < 0.05$; **Figure 1D**). CML-BSA did not significantly affect RAGE expression in DMSO-treated cells, whereas CML-BSA significantly increased RAGE expression in Dox-treated cells, compared to Dox- and DMSO-treated cells (2.43 ± 1.37 -fold, $p < 0.05$, and 3.27 ± 1.95 -fold, $p < 0.01$, respectively; **Figure 1D**). The DMSO did not affect RAGE expression compared to HUVECs cultured in ECM alone (data not shown).

We thus found that Dox increased both endogenous CML formation and RAGE expression in endothelial cells, and the presence of extracellular CML-BSA further increased accumulation of cellular CML and RAGE expression.

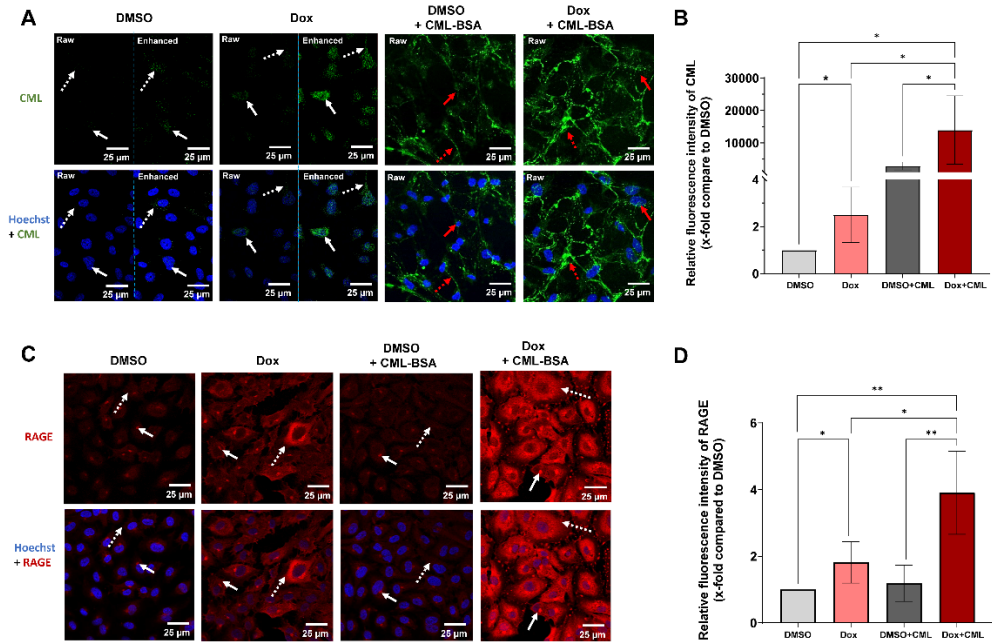


Figure 1. Immunofluorescence staining and quantification of CML and RAGE in HUVECs treated with Dox or/and CML-BSA

Shown are examples of immunofluorescence staining in HUVECs demonstrate the increased accumulation of CML (A) and RAGE (C) following treatment with Dox (10 μ M) or/and exogenous CML-BSA (20 μ g/ml) for 6 h. Endogenous CML was primarily detected in the nucleus and perinuclear regions (white arrows), as well as in the cytoplasm (white dashed arrows), and was visualized in green. Red arrows indicate intracellular CML accumulation, and red dashed arrows indicate intercellular accumulation induced by CML-BSA with/without Dox (A). To visualize the faint signal under Dox-only conditions, fluorescence intensity in the representative Dox/DMSO images was digitally enhanced (right, 'Enhanced'), with the corresponding raw, non-enhanced images shown on the left ('Raw'). Importantly, all quantification in panel (B) was performed on raw, non-enhanced images acquired under identical imaging settings. CML signal intensity was markedly higher under Dox + CML-BSA treatment compared to Dox alone. To enable visualization under Dox-only conditions, RAGE expression was observed as aggregates in the perinuclear regions (white arrows) and the cytoplasm (white dashed arrows), stained in red (C). The nucleic acid was counterstained in blue, as shown in the merged images (the second row), which combine CML/RAGE and nucleic acids staining in endothelial cells. Quantification of fold changes in CML accumulation (B) and RAGE expression (D) was assessed by quantifying the relative fluorescence intensity from immunofluorescence images (in arbitrary units). 15 images per condition were analyzed across four individual experiments (n = 4), using identical imaging settings. The bars in the graphs represent Mean \pm SD. *p<0.05, **p<0.01.

3.2 Effects of Dox and CML-BSA on HUVECs' metabolic viability

The effect of Dox and CML-BSA on endothelial cell viability was determined using an MTT assay (Figure 2), wherein the viability is shown relative to HUVECs cultured in ECM. Treatment with DMSO or DMSO + CML-BSA did not affect

metabolic viability ($99.10 \pm 4.39\%$ and $97.7 \pm 2.81\%$, respectively of ECM cultured HUVECs). In contrast, metabolic viability was significantly reduced to $89.8 \pm 1.88\%$ ($p < 0.001$) in Dox-treated cells and to $88.52 \pm 0.62\%$, in Dox + CML-BSA treated cells ($p < 0.001$), but did not differ significantly between these treatments (**Figure 2**).

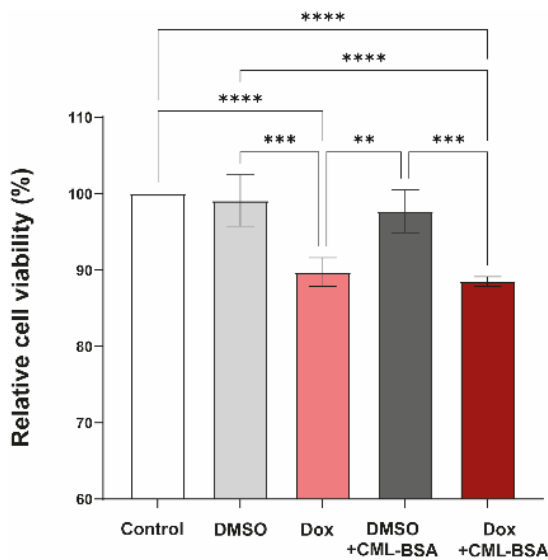


Figure 2. Influence of CML-BSA and Dox on HUVECs' metabolic viability

Quantification of metabolic viability in HUVECs treated with Dox ($10 \mu\text{M}$) or/and exogenous CML-BSA ($20 \mu\text{g/ml}$) for 6 h. Cell viability was measured using the MTT assay (absorbance in arbitrary units), and was normalized to HUVECs cultured in ECM (control, 100% viability), with three replicates per condition in each of three individual experiments ($n = 3$). The bars in the graphs represent Mean \pm SD. ** $p < 0.01$, *** $p < 0.001$, **** $p < 0.0001$.

3.3 Effects of Dox and CML-BSA on oxidative and nitrosative stress in HUVECs

Superoxide production was visualized in live cells using a fluorogenic probe. Superoxide was localized in the cytoplasm, predominantly in the peri-nuclear region (**Figure 3A**). The average superoxide levels after Dox treatment were approximately 1.46 ± 0.55 -fold higher than after DMSO treatment, without reaching statistical significance (**Figure 3B**). Similarly, superoxide levels after DMSO + CML-BSA treatment, did not differ significantly compared to DMSO-treated cells. However, Dox + CML-BSA treatment induced a significant increase in intracellular superoxide levels compared to DMSO + CML-BSA treatment (2.28 ± 0.18 -fold, $p < 0.001$) and sole DMSO treatment (2.08 ± 0.66 -fold, $p < 0.01$) (**Figure 3B**).

As oxidative stress can lead to nitrosative stress^[42], the effects of Dox and CML-BSA on cellular Nitrotyrosine (NT) formation were analyzed. Immunofluorescence analysis showed that NT was localized in the cytoplasm and especially at the plasma membrane (**Figure 3C**). Dox induced a significant 1.84 ± 0.84 -fold increase of cellular NT levels, compared to DMSO-treated cells ($p < 0.05$). In addition, although

CML-BSA itself did not significantly increase NT levels, it significantly exacerbated the Dox-induced increase in NT generation to 2.66 ± 0.83 -fold higher than in DMSO-treated cells ($p < 0.001$) and 1.49 ± 0.23 -fold higher than in cells treated with Dox alone ($p < 0.05$) (**Figure 3D**).

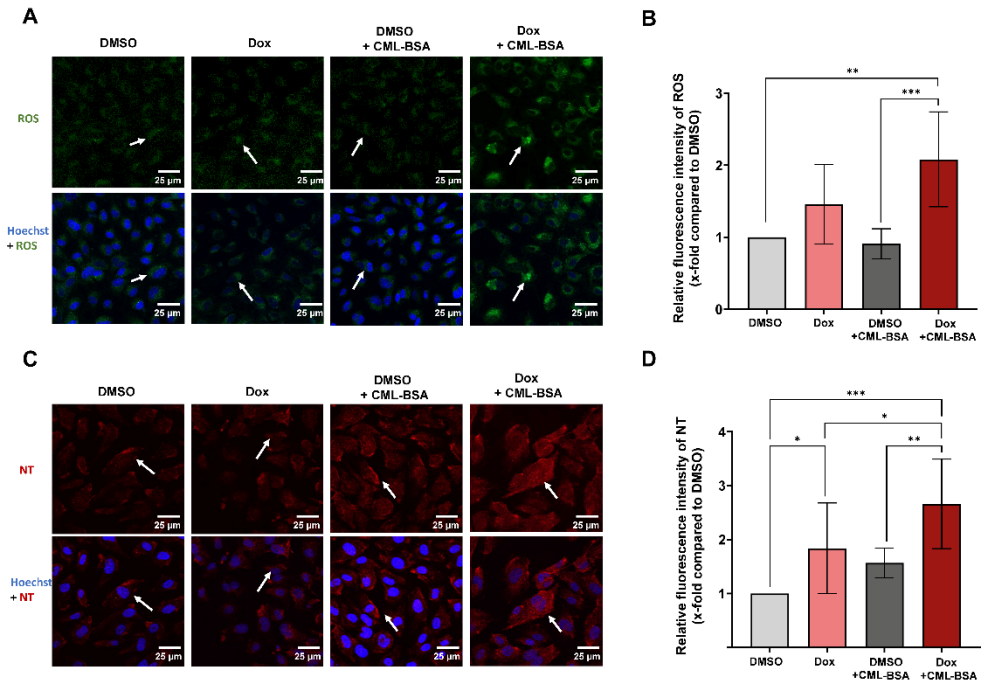


Figure 3. CML-BSA and Dox-Induced oxidative and nitrosative stress in HUVECs

Shown are examples of immunofluorescence staining in HUVECs, highlighting the elevation of ROS and NT in HUVECs treated with Dox (10 μ M) or/and exogenous CML-BSA (20 μ g/ml) for 6 h. ROS expression was concentrated surrounding the nucleus and was stained green as indicated by white arrows in panel A; NT expression was prominently seen at the periphery of the cell membrane and was stained red as indicated by white arrows in panel C; The nucleic acid were stained as blue, as shown in the second row, which are the merge of ROS/NT and nucleic acids in endothelial cells. Quantification of fold changes in ROS (**B**) and NT (**D**) expression in HUVECs were assessed by quantifying the relative fluorescence intensity from immunofluorescence images (in arbitrary units), with 12 images analyzed per condition in each of six individual experiments ($n = 6$). The bars in the graphs represent Mean \pm SD. * $p < 0.05$, ** $p < 0.01$, *** $p < 0.001$.

3.4 Effects of Dox and CML-BSA on NOX5 expression in HUVECs

We then aimed to determine whether the Dox + CML-BSA-induced oxidative/nitrosative stress coincided with an increase in NOX5 expression. Similar to the superoxide levels, a non-significant increase in NOX5 levels was observed in HUVECs treated with Dox (**Figure 4B**). In addition, Dox + CML-BSA induced a significant 1.81 ± 0.13 folds increase in cellular NOX5 levels compared to DMSO-

and DMSO + CML-BSA-treated cells ($p < 0.01$), with a notable enhancement in cytoplasmic NOX5 expression (**Figure 4A and B**).

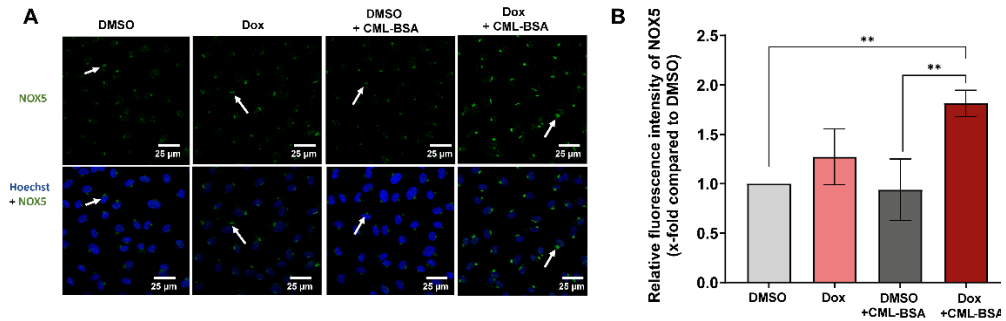


Figure 4. CML-BSA and Dox-Induced NOX5 upregulation in HUVECs

Shown are examples of immunofluorescence staining of NOX5 in HUVECs treated with Dox (10 μ M) and exogenous CML-BSA (20 μ g/ml) for 6 h. NOX5, primarily located adjacent to the nucleus and forming aggregates, was stained green as indicated by white arrows (A). The nucleic acid was stained as blue, as shown in the second row, which are the merge of NOX5 and nucleic acids in endothelial cells. Quantification of fold changes in NOX5 expression was assessed by quantifying the relative fluorescence intensity from immunofluorescence images (in arbitrary units), with 12 images analyzed per condition in each of six individual experiments ($n = 6$). The bars in the graphs represent Mean \pm SD. ** $p < 0.01$.

NOX5 was located in a limited area of the perinuclear region. Interestingly, colocalization with the Golgi apparatus marker cis-Golgi matrix protein 1 (GM130), revealed that NOX5 was predominantly located in the Golgi apparatus (**Figure 5A**) in HUVECs. In contrast, staining with the Endoplasmic Reticulum marker Calreticulin did not show notable colocalization. (**Figure 5B**). Comparison of the NOX5 and GM130 signal between DMSO and Dox-treated cells revealed that the Golgi apparatus appeared to be fragmented after Dox-treatment (**Figure 5A**). Transmission electron microscopy analysis indeed confirmed these Dox-induced structural changes in Golgi apparatus, such as membrane elongation, fragmentation, and deformation (**Figure 5C**).

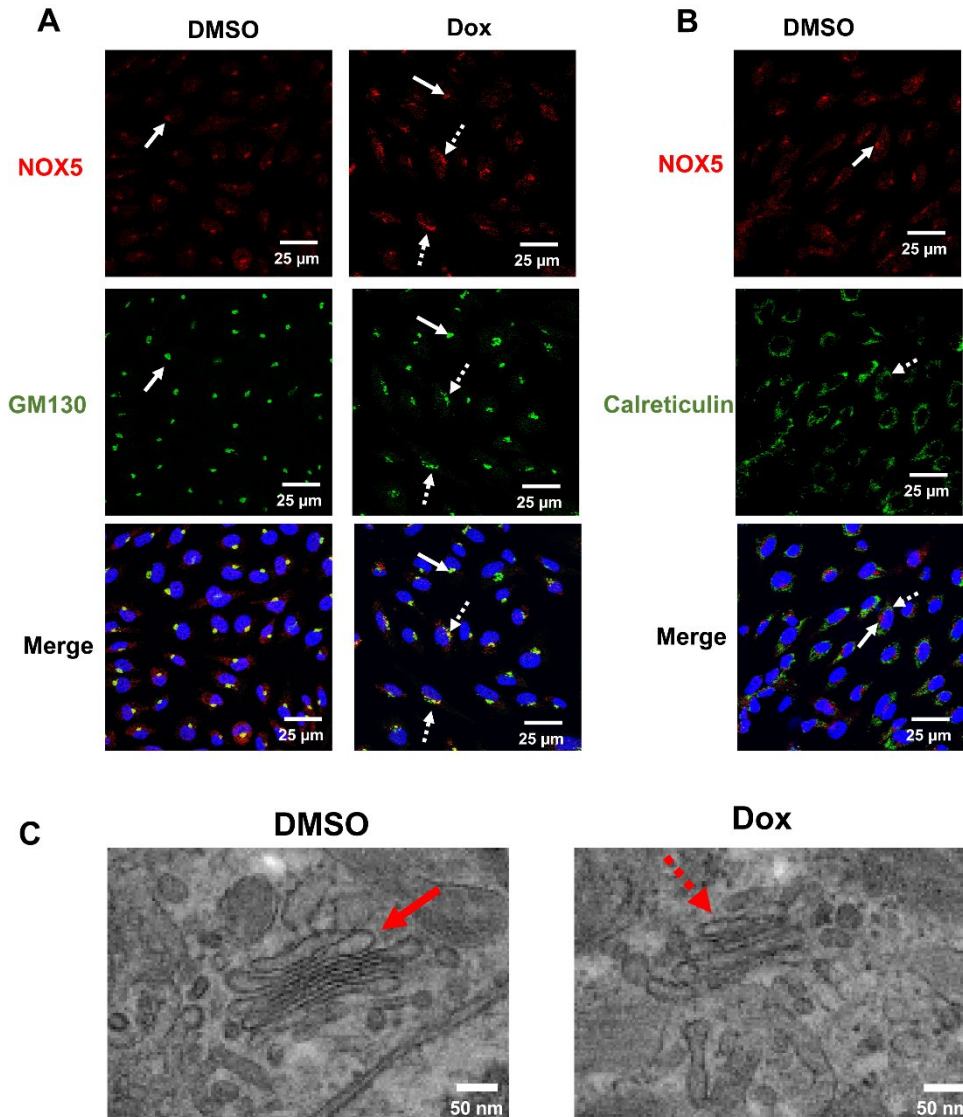


Figure. 5 NOX5 subcellular location and Dox-Induced NOX5 Golgi apparatus fragmentation in HUVECs

Shown are comparison of immunofluorescence double staining for NOX5 and GM130 in HUVECs with/without Dox (10 μ M) treatment for 6 h (A). Panel B presented examples of immunofluorescence double staining for NOX5 and Calreticulin in HUVECs. NOX5 was visualized in red as indicated by white arrows in the first row, while GM130, as the biomarker of Golgi apparatus, was stained as green as shown in the second row (A). Calreticulin, as the biomarker of endoplasmic reticulum, was stained as green as shown in the second row (B). The images shown in the third row are the merge of NOX5, GM130/Calreticulin and blue stained nucleic acids. Arrows in panel A highlight the co-localization of NOX5 and GM130, indicated by the yellow merged, in which, white arrows indicate the normal Golgi apparatus in cells, while white dashed arrows indicates the fragmentation of Golgi apparatus. White arrows in panel B indicates the NOX5 in cells, while white dashed arrows indicate the calreticulin.

Per condition 12 images were analyzed in each of 3 individual experiments ($n = 3$). Panel C illustrates electron microscopy images of Dox-induced Golgi apparatus fragmentation in HUVECs. The red arrows point the normal Golgi apparatus in HUVECs, the red dashed arrows indicate Golgi apparatus fragmentation in HUVECs exposed to Dox ($10 \mu\text{M}$) for 6 h.

3.5 Effects of NOX5 inhibition on Dox- and CML-BSA-induced oxidative and nitrosative stress and RAGE expression in HUVECs

To determine the contribution of NOX5 activity to the observed oxidative- and nitrosative stress, HUVECs were treated with Dox and CML-BSA, either or not in the presence of NOX5 inhibitor ML090^[37].

ML090 lowered superoxide levels in DMSO-treated (0.50 ± 0.16 -fold) as well as Dox-treated cells (0.37 ± 0.04 -fold compared to Dox; $p < 0.05$) (**Figure 6A**). Again, Dox + CML-BSA treatment increased the superoxide level in HUVECs (2.08 ± 0.66 -fold compared to DMSO; $p < 0.001$), which was significantly reduced (0.57 ± 0.04 -fold) in the presence of ML090 ($p < 0.01$).

With respect to nitrosative stress, the presence of ML090 did not significantly affect the Dox-induced NT levels in HUVECs but did reduce NT accumulation induced by Dox + CML-BSA treatment (0.54 ± 0.12 -fold; $p < 0.05$) (**Figure 6B**).

ML 090 did not exhibit a significant effect on mitigating the Dox-induced upregulation of RAGE. However, it did suppress the increase in RAGE expression induced by Dox + CML-BSA treatment (0.53 ± 0.20 -fold; $p < 0.05$) (**Figure 6C**).

Lastly, the significant increase in NOX5 expression by Dox + CML-BSA treatment was significantly inhibited by ML090 (0.50 ± 0.01 - fold) $p < 0.05$) (**Figure 6D**).

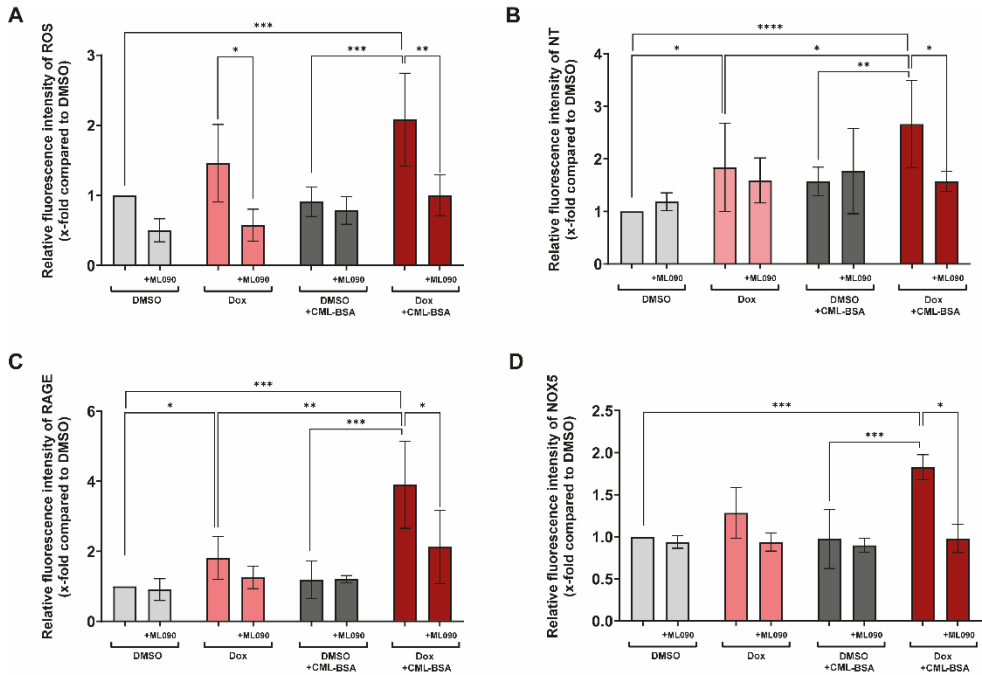


Figure. 6 NOX5 inhibition reduce Dox- and CML-BSA-induced oxidative and nitrosative stress and RAGE expression in HUVECs

Shown are fold changes in oxidative stress biomarker ROS (A), nitrosative stress biomarker NT (B) and RAGE expression (C), as well as NOX5 expression (D) in HUVECs treated with Dox (10 μ M) or/and exogenous CML-BSA (20 μ g/ml) for 6 h, either or not in the presence of NOX5 inhibitor ML090. NT, ROS, RAGE and NOX5 were assessed by quantifying the relative fluorescence intensity from immunofluorescence images (in arbitrary units), with 8 images analyzed per condition in each of three individual experiments ($n = 3$). The bars in the graphs represent Mean \pm SD. * $p < 0.05$, ** $p < 0.01$, *** $p < 0.001$, **** $p < 0.0001$.

4. Discussion

In this study, we investigated the effects of Dox and exogenous CML-BSA on cellular CML levels, RAGE expression and oxidative/nitrosative stress in EC. We found that extracellular added CML-BSA exacerbated Dox-induced CML accumulation, oxidative/nitrosative stress, and RAGE expression in EC. Moreover, an important role herein was found for NOX5 as its expression was increased by Dox and CML-BSA, and NOX5 inhibition alleviated the oxidative/nitrosative stress and RAGE upregulation induced by Dox and CML-BSA.

Dox treatment led to an increase in cellular CML levels in EC, indicative of Dox-induced CML formation. As the formation of AGEs is intrinsically linked to oxidative stress^[12,13], this CML formation might therefore be related to the observed

Dox-induced oxidative stress, as indicated by the increased superoxide levels. Furthermore, oxidative stress is linked to nitrosative stress. Excessive ROS can inhibit endothelial nitric oxide synthase (eNOS) expression in endothelial cells and increase nitric oxide (NO) consumption, thereby reducing NO bioavailability^[10,43]. As NO has been shown to inhibit AGE formation^[44], the observed nitrosative stress may therefore have contributed to the Dox-induced CML formation. Although cellular NO levels were not measured in this study, reduced eNOS expression and NO levels in EC exposed to Dox have been consistently confirmed in multiple studies^[7,10,45,46]. We therefore discuss this mechanism as a plausible explanation supported by the literature, rather than a direct finding of the present work. Moreover, Dox treatment led to increased RAGE expression in EC, which through interaction with CML can exacerbate AGE formation and oxidative stress and EC dysfunction^[12,13], reflecting CML modification rather than albumin, as 10% serum already provided excess BSA compared to the added 20 µg/ml CML-BSA. Together these results indicate that exposure to Dox activates the AGE-RAGE-oxidative stress axis in EC that may be an important mechanism in the pathophysiology of premature vascular ageing and cardiovascular toxicity induced by anthracycline treatment. This is supported by observations in tumor-bearing mice wherein blockage of RAGE with FPS-ZM1 or RAGE knockout reduced Dox-induced cardiac damage and function loss^[47], and in rats wherein treatment with AGE formation inhibitors aminoguanidine and pyridoxamine ameliorated dox-induced cardiac oxidative stress and function loss^[20].

We found that the presence of CML-BSA together with Dox significantly exacerbated the cellular accumulation of CML, oxidative and nitrosative stress and RAGE expression in EC. These important observations are in line with recent observations in human cardiomyocytes *in vitro*, where pre-exposure to AGEs increased exacerbated Dox-induced toxic effects, such as apoptosis and IL-6 production^[48]. However, in their study CML-BSA increased Dox-induced cardiomyocyte apoptosis, whereas we did not observe an additional effect of CML-BSA on Dox-induced cell viability decline. This difference may be related to the differences in AGEs- and Dox treatment protocol (pre-exposure versus simultaneous exposure), incubation time or cell type. Importantly, although CML-BSA did not further reduce cell viability, the observed exacerbation of CML accumulation, oxidative/nitrosative stress, and RAGE expression remains biologically significant. Such sub-lethal alterations can impair endothelial function,

by promoting endothelial activation and enhancing vascular inflammation^[49]. These early dysfunctions may therefore represent an important mechanism through which elevated CML levels contribute to long-term vascular complications during anthracycline therapy. Regardless, this phenomenon indicates that patients with high levels of plasma CML may have an increased risk of (cardio)vascular complications from anthracycline treatment. For instance, in individuals with diabetes, baseline serum CML levels are significantly higher than in non-diabetic individuals, and type 2 diabetes was found to be a key risk factor for the development of late-onset heart failure after anthracycline treatment^[50]. In addition, survival and heart function after Dox treatment were significantly reduced in db/db mice compared to non-diabetic db/+ control mice^[51]. Albeit, in these studies the putative involvement of plasma AGEs herein was not studied. Interestingly, significantly elevated plasma AGE levels were measured at least 5 years after anthracycline treatment in survivors of childhood acute lymphoblastic leukemia and Hodgkin lymphoma compared to healthy age/sex-matched controls^[52,53]. These studies indicate that anthracycline-induced AGE formation may be long-lasting and could be a factor in the long-lasting increased cardiovascular risk associated with this cancer therapy.

Another important and novel observation in this study was the crucial role of NOX5 in the observed Dox + CML-BSA-induced effects in EC. Dox, especially in the presence of CML-BSA, increased NOX5 expression and inhibition of NOX5 with ML090 effectively reduced Dox + CML-BSA-induced superoxide and nitrotyrosine levels and RAGE expression. The used dose was based on a recent dose-finding study of NOX inhibitors, showing that a dose of 0.01 μM most potently and selectively inhibited NOX5^[37]. Our findings using ML090 therefore provide supportive, but not definitive, evidence of NOX5 involvement. Increased expression of NOX5 in EC has been shown in different pathologies, such as in the cardiac microvasculature of myocardial infarction patients^[28] and COVID-19 patients^[29]. Moreover, we found NOX5 to be primarily localized in the Golgi apparatus of EC. Interestingly, The Golgi is an important cellular compartment for eNOS activity in EC^[54] and a relation between NOX5 and eNOS activity has been shown. Notably, impaired endothelium-dependent vasodilation due to uncoupled eNOS was found in mice expressing human NOX5 in endothelial cells^[55], whereas in another study, NOX5 was paradoxically found to activate eNOS in blood vessel endothelium^[56]. However, how these findings relate to our observed effects of NOX5 inhibition on Dox-induced oxidative and nitrosative stress and the exact role of NOX5 in the

Golgi herein remain to be elucidated. The key role of NOX5 in Dox-induced EC dysfunction however, suggests it may be a suitable target for therapy to limit anthracyclin-induced cardiovascular complications.

Lastly, we observed fragmentation of the Golgi in EC exposed to Dox. Dox-induced apoptosis in endothelial cells has been widely reported, while Golgi fragmentation is recognized as a significant marker of apoptotic stress and can be the result of oxidative stress^[7,57-59]. Whether ROS production by NOX5, which we found localized primarily in the Golgi in EC, contributes to its fragmentation remains to be established, for instance through NOX5 inhibition or knockdown. Moreover, at present we cannot explain the mechanisms underlying the relationship between the Golgi-located NOX5 and the observed Dox-induced effects on RAGE expression and CML accumulation. Answers to these questions will require future NOX5-targeted validations to elucidate causality and mechanisms.

In conclusion, this study demonstrated that extracellular CML-BSA significantly exacerbates Dox-induced oxidative/nitrosative stress and RAGE activation in endothelial cells, which could be significantly counteracted by NOX5 inhibition. These findings provided novel insights into the mechanisms underlying Dox-induced endothelial dysfunction and suggest potential therapeutic targets for mitigating the cardiovascular side effects of anthracycline chemotherapy. Of note, although in this study we focussed on CML, other AGEs have been found to be induced by Dox^[20] and we can therefore not rule out roles for other AGEs in Dox-induced vascular toxicity also.

Acknowledgments of grant support:

This work was supported by the China Scholarship Council (Beijing, China, grant number 202008320278 to ZJ);

Author contributions

Zhu Jiang: Data curation; Formal analysis; Funding acquisition; Investigation; Methodology; Software; Validation; Visualization; Writing - original draft; **Ingeborg.S.E.Waas:** Data curation; Formal analysis; Visualization; Writing - review; **Suat Simsek:** Resources; Methodology; Writing - review; **Casper G. Schalkwijk:** Resources; Writing - review; **Joris J.T.H. Roelofs:** Supervision; writing - review; **Hans W.M. Niessen:** Resources; Project administration; Conceptualization; Funding acquisition; Methodology; Supervision; Writing -

review; **Paul A.J. Krijnen**: Resources; Project administration; Conceptualization; Funding acquisition; Methodology; Supervision; Writing - review & editing;

Competing Interest

The authors declare no competing interests.

Disclosure

None

References

- [1]. Rivankar S. An overview of doxorubicin formulations in cancer therapy. *J Cancer Res Ther.* 2014;10:853–858. doi: 10.4103/0973-1482.139267
- [2]. Swain SM, Whaley FS, Ewer MS. Congestive heart failure in patients treated with doxorubicin: a retrospective analysis of three trials. *Cancer.* 2003;97:2869–2879. doi: 10.1002/cncr.11407
- [3]. Zamorano JL, Lancellotti P, Muñoz DR, Aboyans V, Asteggiano R, Galderisi M, Habib G, Lenihan DJ, Lip GY, Lyon AR, et al. [2016 ESC Position Paper on cancer treatments and cardiovascular toxicity developed under the auspices of the ESC Committee for Practice Guidelines]. *Kardiol Pol.* 2016;74:1193–1233. doi: 10.5603/kp.2016.0156
- [4]. Bloom MW, Hamo CE, Cardinale D, Ky B, Nohria A, Baer L, Skopicki H, Lenihan DJ, Gheorghiadu M, Lyon AR, et al. Cancer Therapy-Related Cardiac Dysfunction and Heart Failure: Part 1: Definitions, Pathophysiology, Risk Factors, and Imaging. *Circ Heart Fail.* 2016;9:e002661. doi: 10.1161/CIRCHEARTFAILURE.115.002661
- [5]. Smith LA, Cornelius VR, Plummer CJ, Levitt G, Verrill M, Canney P, Jones A. Cardiotoxicity of anthracycline agents for the treatment of cancer: systematic review and meta-analysis of randomised controlled trials. *BMC cancer.* 2010;10:1–14.
- [6]. Soultati A, Mountzios G, Avgerinou C, Papaxoinis G, Pectasides D, Dimopoulos MA, Papadimitriou C. Endothelial vascular toxicity from chemotherapeutic agents: preclinical evidence and clinical implications. *Cancer Treat Rev.* 2012;38:473–483. doi: 10.1016/j.ctrv.2011.09.002
- [7]. Sonowal H, Pal P, Shukla K, Saxena A, Srivastava SK, Ramana KV. Aldose reductase inhibitor, fidarestat prevents doxorubicin-induced endothelial cell death and dysfunction. *Biochem Pharmacol.* 2018;150:181–190. doi: 10.1016/j.bcp.2018.02.018
- [8]. Tsai TH, Lin CJ, Hang CL, Chen WY. Calcitriol Attenuates Doxorubicin-Induced Cardiac Dysfunction and Inhibits Endothelial-to-Mesenchymal Transition in Mice. *Cells.* 2019;8. doi: 10.3390/cells8080865
- [9]. Wojcik T, Szczesny E, Chlopicki S. Detrimental effects of chemotherapeutics and other drugs on the endothelium: A call for endothelial toxicity profiling. *Pharmacol Rep.* 2015;67:811–817. doi: 10.1016/j.pharep.2015.03.022
- [10]. Kalivendi SV, Kotamraju S, Zhao H, Joseph J, Kalyanaraman B. Doxorubicin-induced apoptosis is associated with increased transcription of endothelial nitric-oxide synthase. Effect of antiapoptotic antioxidants and calcium. *J Biol Chem.* 2001;276:47266–47276. doi: 10.1074/jbc.M106829200
- [11]. Schleicher ED, Wagner E, Nerlich AG. Increased accumulation of the glycoxidation product N (epsilon)-(carboxymethyl) lysine in human tissues in diabetes and aging. *The Journal of clinical investigation.* 1997;99:457–468.
- [12]. Ren X, Ren L, Wei Q, Shao H, Chen L, Liu N. Advanced glycation end-products decreases expression of endothelial nitric oxide synthase through oxidative stress in human coronary artery endothelial cells. *Cardiovascular Diabetology.* 2017;16:52. doi: 10.1186/s12933-017-0531-9
- [13]. Yan SD, Schmidt AM, Anderson GM, Zhang J, Brett J, Zou YS, Pinsky D, Stern D. Enhanced cellular oxidant stress by the interaction of advanced glycation end products with their receptors/binding proteins. *Journal of Biological Chemistry.* 1994;269:9889–9897. doi: [https://doi.org/10.1016/S0021-9258\(17\)36966-1](https://doi.org/10.1016/S0021-9258(17)36966-1)

- [14]. Fuijkschot WW, de Graaff HJ, Berishvili E, Kakabadze Z, Kupreishvili K, Meinster E, Houtman M, van Broekhoven A, Schalkwijk CG, Vonk AB, et al. Prevention of age-induced N(ε)-(carboxymethyl)lysine accumulation in the microvasculature. *Eur J Clin Invest*. 2016;46:334–341. doi: 10.1111/eci.12599
- [15]. Schleicher ED, Wagner E, Nerlich AG. Increased accumulation of the glycooxidation product N(ε)-(carboxymethyl)lysine in human tissues in diabetes and aging. *J Clin Invest*. 1997;99:457–468. doi: 10.1172/jci119180
- [16]. Hanssen NM, Beulens JW, van Dieren S, Scheijen JL, van der AD, Spijkerman AM, van der Schouw YT, Stehouwer CD, Schalkwijk CG. Plasma advanced glycation end products are associated with incident cardiovascular events in individuals with type 2 diabetes: a case-cohort study with a median follow-up of 10 years (EPIC-NL). *Diabetes*. 2015;64:257–265. doi: 10.2337/db13-1864
- [17]. Del Turco S, Basta G. An update on advanced glycation endproducts and atherosclerosis. *Biofactors*. 2012;38:266–274. doi: 10.1002/biof.1018
- [18]. Wang Z, Jiang Y, Liu N, Ren L, Zhu Y, An Y, Chen D. Advanced glycation end-product Nε-carboxymethyl-Lysine accelerates progression of atherosclerotic calcification in diabetes. *Atherosclerosis*. 2012;221:387–396. doi: 10.1016/j.atherosclerosis.2012.01.019
- [19]. Bruynzeel AM, Abou El Hassan MA, Schalkwijk C, Berkhof J, Bast A, Niessen HW, van der Vijgh WJ. Anti-inflammatory agents and monoHER protect against DOX-induced cardiotoxicity and accumulation of CML in mice. *Br J Cancer*. 2007;96:937–943. doi: 10.1038/sj.bjc.6603640
- [20]. Moriyama T, Kemi M, Okumura C, Yoshihara K, Horie T. Involvement of advanced glycation end-products, pentosidine and N(ε)-(carboxymethyl)lysine, in doxorubicin-induced cardiomyopathy in rats. *Toxicology*. 2010;268:89–97. doi: 10.1016/j.tox.2009.12.004
- [21]. Haesen S, Jager MM, Brillouet A, de Laat I, Vastmans L, Verghote E, Delaet A, D’Haese S, Hamad I, Kleinewietfeld M, et al. Pyridoxamine Limits Cardiac Dysfunction in a Rat Model of Doxorubicin-Induced Cardiotoxicity. *Antioxidants*. 2024;13:112.
- [22]. Clayton ZS, Brunt VE, Hutton DA, Casso AG, Ziemba BP, Melov S, Campisi J, Seals DR. Tumor Necrosis Factor Alpha-Mediated Inflammation and Remodeling of the Extracellular Matrix Underlies Aortic Stiffening Induced by the Common Chemotherapeutic Agent Doxorubicin. *Hypertension*. 2021;77:1581–1590. doi: 10.1161/HYPERTENSIONAHA.120.16759
- [23]. Quagliariello V, Paccone A, Iovine M, Buccolo S, Maurea N. P131 LOW DOSES OF ADVANCED GLYCATION END-PRODUCTS AND FRUCTOSILATION PRODUCTS PROMOTES PREMATURE CELL DEATH OF HUMAN CARDIAC CELLS EXPOSED TO DOXORUBICIN VIA ACTIVATION OF NLRP3, MYD88 AND P53 DOWNREGULATION. *European Heart Journal Supplements*. 2022;24. doi: 10.1093/eurheartj/suac012.127
- [24]. Ikeda A, Wang G, Korolowicz K, Rodriguez O, Hudson B, Bishopric NH. THE RECEPTOR FOR ADVANCED GLYCATION ENDPRODUCTS AMPLIFIES DOXORUBICIN CARDIOTOXICITY. *JACC*. 2024;83:366–366. doi: 10.1016/S0735-1097(24)02356-8
- [25]. Drummond GR, Sobey CG. Endothelial NADPH oxidases: which NOX to target in vascular disease? *Trends in Endocrinology & Metabolism*. 2014;25:452–463. doi: <https://doi.org/10.1016/j.tem.2014.06.012>
- [26]. Wautier MP, Chappey O, Corda S, Stern DM, Schmidt AM, Wautier JL. Activation of NADPH oxidase by AGE links oxidant stress to altered gene expression via RAGE. *Am J Physiol Endocrinol Metab*. 2001;280:E685–694. doi: 10.1152/ajpendo.2001.280.5.E685
- [27]. Guzik TJ, Chen W, Gongora MC, Guzik B, Lob HE, Mangalat D, Hoch N, Dikalov S, Rudzinski P, Kapelak B, et al. Calcium-dependent NOX5 nicotinamide adenine dinucleotide phosphate oxidase contributes to vascular oxidative stress in human coronary artery disease. *J Am Coll Cardiol*. 2008;52:1803–1809. doi: 10.1016/j.jacc.2008.07.063
- [28]. Hahn NE, Meischl C, Kawahara T, Musters RJ, Verhoef VM, van der Velden J, Vonk AB, Paulus WJ, van Rossum AC, Niessen HW, et al. NOX5 expression is increased in intramyocardial blood vessels and cardiomyocytes after acute myocardial infarction in humans. *Am J Pathol*. 2012;180:2222–2229. doi: 10.1016/j.ajpath.2012.02.018
- [29]. Jiang Z, Wu L, van der Leeden B, van Rossum AC, Niessen HWM, Krijnen PAJ. NOX2 and NOX5 are increased in cardiac microvascular endothelium of deceased COVID-19 patients. *Int J Cardiol*. 2023;370:454–462. doi: 10.1016/j.ijcard.2022.10.172
- [30]. Marqués J, Fernández-Irigoyen J, Ainzúa E, Martínez-Azcona M, Cortés A, Roncal C, Orbe J, Santamaría E, Zalba G. NADPH Oxidase 5 (NOX5) Overexpression Promotes Endothelial Dysfunction via Cell Apoptosis, Migration, and Metabolic Alterations in Human Brain Microvascular Endothelial Cells

- (hCMEC/D3). *Antioxidants*. 2022;11. doi: 10.3390/antiox11112147
- [31]. Kislinger T, Fu C, Huber B, Qu W, Taguchi A, Du Yan S, Hofmann M, Yan SF, Pischetsrieder M, Stern D, et al. N(epsilon)-(carboxymethyl)lysine adducts of proteins are ligands for receptor for advanced glycation end products that activate cell signaling pathways and modulate gene expression. *J Biol Chem*. 1999;274:31740–31749. doi: 10.1074/jbc.274.44.31740
- [32]. Thornalley PJ, Battah S, Ahmed N, Karachalias N, Agalou S, Babaei-Jadidi R, Dawnay A. Quantitative screening of advanced glycation endproducts in cellular and extracellular proteins by tandem mass spectrometry. *Biochem J*. 2003;375:581–592. doi: 10.1042/bj20030763
- [33]. Pirkmajer S, Chibalin AV. Serum starvation: caveat emptor. *Am J Physiol Cell Physiol*. 2011;301:C272–279. doi: 10.1152/ajpcell.00091.2011
- [34]. Boehm BO, Schilling S, Rosinger S, Lang GE, Lang GK, Kientsch-Engel R, Stahl P. Elevated serum levels of Nε-carboxymethyl-lysine, an advanced glycation end product, are associated with proliferative diabetic retinopathy and macular oedema. *Diabetologia*. 2004;47:1376–1379. doi: 10.1007/s00125-004-1455-y
- [35]. Semba RD, Najjar SS, Sun K, Lakatta EG, Ferrucci L. Serum Carboxymethyl-Lysine, an Advanced Glycation End Product, Is Associated With Increased Aortic Pulse Wave Velocity in Adults. *American Journal of Hypertension*. 2009;22:74–79. doi: 10.1038/ajh.2008.320
- [36]. Francis GL. Albumin and mammalian cell culture: implications for biotechnology applications. *Cytotechnology*. 2010;62:1–16. doi: 10.1007/s10616-010-9263-3
- [37]. Dao VT, Elbatreek MH, Altenhofer S, Casas AI, Pachado MP, Neullens CT, Knaus UG, Schmidt H. Isoform-selective NADPH oxidase inhibitor panel for pharmacological target validation. *Free Radic Biol Med*. 2020;148:60–69. doi: 10.1016/j.freeradbiomed.2019.12.038
- [38]. Baidoshvili A, Krijnen PA, Kupreishvili K, Ciurana C, Bleeker W, Nijmeijer R, Visser CA, Visser FC, Meijer CJ, Stooker W, et al. N(epsilon)-(carboxymethyl)lysine depositions in intramyocardial blood vessels in human and rat acute myocardial infarction: a predictor or reflection of infarction? *Arterioscler Thromb Vasc Biol*. 2006;26:2497–2503. doi: 10.1161/01.ATV.0000245794.45804.ab
- [39]. Mosmann T. Rapid colorimetric assay for cellular growth and survival: Application to proliferation and cytotoxicity assays. *Journal of Immunological Methods*. 1983;65:55–63. doi: [https://doi.org/10.1016/0022-1759\(83\)90303-4](https://doi.org/10.1016/0022-1759(83)90303-4)
- [40]. van Tonder A, Joubert AM, Cromarty AD. Limitations of the 3-(4,5-dimethylthiazol-2-yl)-2,5-diphenyl-2H-tetrazolium bromide (MTT) assay when compared to three commonly used cell enumeration assays. *BMC Research Notes*. 2015;8:47. doi: 10.1186/s13104-015-1000-8
- [41]. Mross K, Maessen P, van der Vijgh WJ, Gall H, Boven E, Pinedo HM. Pharmacokinetics and metabolism of epidoxorubicin and doxorubicin in humans. *J Clin Oncol*. 1988;6:517–526. doi: 10.1200/JCO.1988.6.3.517
- [42]. Pacher P, Beckman JS, Liaudet L. Nitric Oxide and Peroxynitrite in Health and Disease. *Physiological Reviews*. 2007;87:315–424. doi: 10.1152/physrev.00029.2006
- [43]. Skrypnik I, Maslova G, Lymanets T, Gusachenko I. L-arginine is an effective medication for prevention of endothelial dysfunction, a predictor of anthracycline cardiotoxicity in patients with acute leukemia. *Experimental oncology*. 2017.
- [44]. Asahi K, Ichimori K, Nakazawa H, Izuahara Y, Inagi R, Watanabe T, Miyata T, Kurokawa K. Nitric oxide inhibits the formation of advanced glycation end products. *Kidney International*. 2000;58:1780–1787. doi: <https://doi.org/10.1111/j.1523-1755.2000.00340.x>
- [45]. Murata T, Yamawaki H, Yoshimoto R, Hori M, Sato K, Ozaki H, Karaki H. Chronic effect of doxorubicin on vascular endothelium assessed by organ culture study. *Life sciences*. 2001;69:2685–2695.
- [46]. Yin Z, Zhao Y, Li H, Yan M, Zhou L, Chen C, Wang DW. miR-320a mediates doxorubicin-induced cardiotoxicity by targeting VEGF signal pathway. *Aging (Albany NY)*. 2016;8:192.
- [47]. Ikeda A, Wang G, Korolowicz K, Rodriguez O, Hudson B, Bishopric NH. THE RECEPTOR FOR ADVANCED GLYCATION ENDPRODUCTS AMPLIFIES DOXORUBICIN CARDIOTOXICITY. *Journal of the American College of Cardiology*. 2024;83:366. doi: [https://doi.org/10.1016/S0735-1097\(24\)02356-8](https://doi.org/10.1016/S0735-1097(24)02356-8)
- [48]. Quagliarriello V, Iovine M, D'Aiuto G, Buccolo S, Maurea C, Bonelli A, Paccone A, Canale ML, Maurea N. Low doses of advanced glycation end-products and fructosilation products promotes premature cell death of human cardiac cells and increases drug resistance of human breast cancer cells exposed to doxorubicin through NLRP3 and MyD88 pathways. *Journal of Clinical Oncology*. 40:e24055–e24055. doi: 10.1200/JCO.2022.40.16_suppl.e24055
- [49]. Heidland A, Sebekova K, Schinzel R. Advanced glycation end products and the progressive course of

- renal disease. *American Journal of Kidney Diseases*. 2001;38:S100–S106. doi: <https://doi.org/10.1053/ajkd.2001.27414>
- [50]. Qin A, Thompson CL, Silverman P. Predictors of late-onset heart failure in breast cancer patients treated with doxorubicin. *Journal of Cancer Survivorship*. 2015;9:252–259. doi: 10.1007/s11764-014-0408-9
- [51]. Pei XM, Tam BT, Sin TK, Wang FF, Yung BY, Chan LW, Wong CS, Ying M, Lai CW, Siu PM. S100A8 and S100A9 Are Associated with Doxorubicin-Induced Cardiotoxicity in the Heart of Diabetic Mice. *Front Physiol*. 2016;7:334. doi: 10.3389/fphys.2016.00334
- [52]. Felicetti F, Cento AS, Fornengo P, Cassader M, Mastrocola R, D'Ascenzo F, Settanni F, Benso A, Arvat E, Collino M, et al. Advanced glycation end products and chronic inflammation in adult survivors of childhood leukemia treated with hematopoietic stem cell transplantation. *Pediatr Blood Cancer*. 2020;67:e28106. doi: 10.1002/pbc.28106
- [53]. Felicetti F, Aimaretti E, Dal Bello F, Gatti F, Godono A, Saba F, Einaudi G, Collino M, Fagioli F, Aragno M, et al. Advanced glycation end products and their related signaling cascades in adult survivors of childhood Hodgkin lymphoma: A possible role in the onset of late complications. *Free Radical Biology and Medicine*. 2022;178:76–82. doi: <https://doi.org/10.1016/j.freeradbiomed.2021.11.036>
- [54]. Villadangos L, Serrador JM. Subcellular Localization Guides eNOS Function. *International Journal of Molecular Sciences*. 2024;25:13402.
- [55]. Elbatreek MH, Sadegh S, Anastasi E, Guney E, Nogales C, Kacprowski T, Hassan AA, Teubner A, Huang PH, Hsu CY, et al. NOX5-induced uncoupling of endothelial NO synthase is a causal mechanism and therapeutic target of an age-related hypertension endotype. *PLoS Biol*. 2020;18:e3000885. doi: 10.1371/journal.pbio.3000885
- [56]. Zhang Q, Malik P, Pandey D, Gupta S, Jagnandan D, Belin de Chantemele E, Banfi B, Marrero MB, Rudic RD, Stepp DW, et al. Paradoxical activation of endothelial nitric oxide synthase by NADPH oxidase. *Arterioscler Thromb Vasc Biol*. 2008;28:1627–1633. doi: 10.1161/atvbaha.108.168278
- [57]. Yang B, Li H, Qiao Y, Zhou Q, Chen S, Yin D, He H, He M. Tetramethylpyrazine Attenuates the Endotheliotoxicity and the Mitochondrial Dysfunction by Doxorubicin via 14-3-3gamma/Bcl-2. *Oxid Med Cell Longev*. 2019;2019:5820415. doi: 10.1155/2019/5820415
- [58]. Wu S, Ko YS, Teng MS, Ko YL, Hsu LA, Hsueh C, Chou YY, Liew CC, Lee YS. Adriamycin-induced cardiomyocyte and endothelial cell apoptosis: in vitro and in vivo studies. *J Mol Cell Cardiol*. 2002;34:1595–1607. doi: 10.1006/jmcc.2002.2110
- [59]. Machamer CE. The Golgi complex in stress and death. *Frontiers in neuroscience*. 2015;9:421.